THREE-DIMENSIONAL MODEL OF NON-LOAD BEARING LSF WALLS UNDER FIRE

Makrem Ameur

Master's degree in construction engineering

Supervised by:

Paulo Piloto
Ismail Yousfi

Bragança 2020

THREE-DIMENSIONAL MODEL OF NON-LOAD BEARING LSF WALLS UNDER FIRE

Makrem Ameur

Dissertation presented to the Escola Superior de Tecnologia e Gestão of Instituto Politécnico de Bragança, made under the Double Diploma agreement of the Polytechnic Institute of Bragança and Tunisia Private University (ULT), to obtain the Master's Degree in Construction Engineering

Bragança 2020

Acknowledgements

I would like to thank the following people who have helped me undertake this dissertation

Firstly, I'd like to express my gratitude to my supervisor, Paulo Piloto who has supported me during the development of my thesis. Also, for the kindness and the spontaneity, for all his feedbacks, his advice so that he motivate me to defend this work. I had the great pleasure of working under his direction, his professional competence as well as his human quality.

I 'd like to express my big and sincere thanks to my supervisor Ismail Yousfi for his consistent support, help and guidance during the running of this project and for the thoughtful comments and recommendations on this dissertation.

I'm also thankful to the members of the juries who agreed to assess my work.

To conclude, I cannot forget to thank my family and friends for all the unconditional support in this very intense academic year.

Abstract

The present work presents numerical study with the aim of analysing the fire performance on LSF non load bearing walls.

Numerical validation of the full-scale fire test developed by Anthony Deloge Ariyanayagam, Mahen Mahendran [1] was developed using transient thermal analysis, assuming perfect contact between different materials to determine the fire insolation criteria (I). The insulation criterion is defined by the average temperature or by the maximum temperature determined on the unexposed side of the wall.

Two extra 3D numerical analysis were developed with the objective of understanding the thermal effect of the cavity size and the number of protection layers.

Two different types of errors were used to compare the numerical and experimental results. The absolute relative error has been applied to compare the fire resistance time obtained by the numerical simulation and the fire test. The Root mean square (RMS) was used to compare the time history temperature error, determined on different locations of the wall section on specific points.

Keywords: LSF walls, Non-load bearing, Fire resistance, Numerical validation, Parametric analysis, Ansys Multiphysics,

Resumo

O presente trabalho apresenta um estudo numérico com o objetivo de analisar o desempenho ao fogo em paredes não estruturais fabricadas em aço enformado a frio LSF. Será apresentada a validação numérica do ensaio experimental de resistência ao fogo, de um modelo em grande escala, desenvolvido por Anthony Deloge Ariyanayagam, Mahen Mahendran [15]. Este objetivo foi alcançado usando uma análise térmica transitória, assumindo contato perfeito entre diferentes materiais. Foi assim possível aplicar o critério de isulamento de fogo (I), determinada pela temperatura média ou pela temperatura máxima determinada do lado não exposto.

Duas simulações numéricas 3D adicionais foram desenvolvidas com o objetivo de se conhecer a influência térmica da espessura da cavidade e a influência do número de camadas de proteção.

A comparação entre os resultados numéricos e experimentais foi realizada com dois métodos. O erro relativo absoluto foi utilizado para comparar o tempo de resistência ao fogo obtido pela simulação numérica e o ensaio experimental. O erro quadrático médio (RMS) foi usado para comparar a evolução da temperatura em diferentes locais da secção da parede para determinados instantes de tempo.

Nomenclature and abbreviations

LSF: Light Steel Framing

FRL: Fire Resistance Level

C_p: Specific heat

λ: Conductivity

ρ: Specific mass

ε: Emissivity

Θ_g: Initial ambient temperature

α_c: Convection coefficient

Pb: Plaster board

CF: Cold flange

HF: Hot flange

RE: Relative error

Contents

List of tables

List of figures

Chapter1: Introduction

1.1. General

Fire safety of light steel frame (LSF) stud wall system is critical to the building design. This element has received an important interest from the building industry and the community during the last years. The light steel frame (LSF) development technology begun to be used in several types of buildings, supplanting the traditional construction strategies due to its light-weight characteristics: steel is reused, dimensional stability, and ease of installation.

Light steel frames are broadly utilized in non-load-bearing walls, with application to different sorts of buildings, such as health buildings, educational buildings, residential buildings and other type of public buildings. The fire protection of the LSF wall requires one or more layers of fire protection materials. The fire tests on non-load-bearing LSF walls begun to be explored in 2017 at the Polytechnic Institute of Braganca (IPB) with the aim of creating accurate numerical models based on the thermal analysis with fluid structure interaction, validating the numerical models with tests performed by others; analysing the fire performance of LSF using the simplified one-dimensional heat flow, presenting an accurate numerical model to consider the fire resistance of LSF walls made with composite panels under ISO standard fire conditions and predict the insulation criteria on the LSF walls.

1.2. Objective of thesis

The main objective of this study is to present the fire resistance on a non-load bearing walls Light Steel Frame (LSF) structure. Compare the performance of the fire resistance with different LSF wall structure or with different materials using a numerical model. In this context, specific tasks are included to be investigated: different LSF structures and steel thicknesses, special numerical tasks need to be developed to get an accurate model to predict fire resistance, using ANSYS multi-physics, the validation should be done with 3D finite element models, and then, a parametric analysis have been developed for getting more clear ideas about the perfect contact between the different materials.

1.3. Plan of thesis

This thesis is divided into 6 chapters. The first chapter contains a brief introduction to present the work, and its objectives. The second chapter consists of the state of the art in the context of results of some research carried out in steel framing concept. The third chapter, named fire resistance in LSF walls, presents the insulation criteria (I) and highlights the required standards to be followed from eurocodes for design and the EN 1363-1 for the experimental tests. The fourth chapter presents the heat transfer approach as well as the three modes of heat transfer: conduction, convection, radiation. The fifth chapter consist of the numerical simulation that includes ANSYS Multi-physics Software, material properties, boundary conditions, numerical validation analysis and the parametric analysis. The sixth chapter presents the conclusion of this thesis, as well as the possible horizons of the project as a proposal for future work.

Chapter 2: State of art

Steel framing has become popular in the recent years in new-build construction because of its properties like the non-combustibility, dimensional stability, ease of installation.

Cold-rolled steel sections and lightweight steel framing (LSF) looks to increase in popularity as new technologies begin to replace the more traditional building methods. Lightweight Steel Framing (LSF) is manufactured using cold formed sheet steel. LSF is used in the wall, floor, and roof assemblies in residences, as well as commercial buildings, including schools, shopping malls, row houses, hotels, assisted care residences, and office buildings.

Sultan, M.A in 1996 [1] did a development and validation of a model for predicting the fire resistance of non-insulated and unloaded steel-stud wall assemblies. In this study, the heat transfer equations, that determine the temperature history across the wall assembly, from the fire side to the ambient side, were programmed, and the program was used to predict the temperature distribution for a given time temperature relationship for the fire and for the gypsum board thicknesses. The wall assemblies were also tested under standard fire-test conditions, and the measured and predicted temperature results were compared. As results from the full-scale test, the model predicts slightly higher temperatures than the temperatures measured by bare thermocouples on the unexposed face. This was probably the result of neglecting moisture migration through the gypsum board to the unexposed side. The comparisons show that the model provides reasonable conservative fire resistance predictions (approximately 3% lower than the measured fire-resistance rating). Gypsum board is no longer in place when its temperature exceeds 600°C. However, the model considers that the membrane remains in place until assembly. The model predicts the temperatures across non-insulated wall assemblies generally well compared to the measured temperatures. Further studies will address the effect of insulation in the wall cavity and the addition of structural loads to the assemblies. The model predicts slightly conservative fire-resistance ratings compared to the experimental measurements. This is appropriate for most fire safety engineering applications [1].

Sultan's full-scale fire resistance tests on non-load bearing LSF wall assemblies showed that, when rock wool was used as cavity insulation, the fire resistance rating (FRR) increased by 54% over the non-insulated wall assemblies while glass fibre did not affect the fire performance. He also found that cellulose fibre cavity insulation reduced the FRR [1].

In 1999 the National Research Council of Canada (NRC), in partnership with the North American steel industry, did a report about the previous and current experimental and analytical study on the fire resistance of load bearing cold-formed steel-framed wall and floor assemblies[2].

Harmathy and Sultan studied the correlation between the severity of ASTM El I9 and IS0 834 fire exposures and found that the IS0 test is slightly less severe but that differences in the fire endurance values the two tests yielded should not be expected to exceed 5 minutes [2].

Son and Shoub described two fire-endurance tests on double-wall assemblies. In both tests, the assemblies consisted of two LSF walls of similar design separated by the cavity, the inner and outer surfaces were of gypsum board but with different thick type X. The first assembly was constructed of "C" shaped stud with glass fibre insulation. And the second one used the rectangular tube stud with glass fibre insulation to fit the wall cavity. In the first test, structural failure of the fire-exposed wall was seen at 42 minutes, 1 minute after a considerable part of the fire-exposed gypsum board fell away. In the second, the fire-exposed wall experienced structural failure at 67 minutes, and the gypsum board started falling at 48 minutes. The second test showed much slower heat penetration through the wall assembly, which was attributed to thicker insulation [2].

Klippstein did an experimental study of nine wall assemblies, seven non-insulated and two insulated, were tested for fire endurance under various load intensities. And another three fire tests on loadbearing insulated LSF walls, all the walls were typically consisted of six C-shaped steel studs, with the same cross-sectional dimensions except one wall, with stiffening lips with up to three layers of fire-resistant gypsum board thick on each side. The two last walls have less high than the others to accommodate load cells under the centre line of each stud to monitor axial loads. During the latter phase, the total load was redistributed to the studs farther away from the centre of the wall. The load cell data also indicated that the total load applied to wall assemblies was not stable during fire tests and usually exceeded by up to 100% the intended load level. Klippstein advocated

changing standard fire test procedures to ensure uniformity in steel stud behaviour and reproducibility of fire test results [2].

Gerlich, Collier, and Buchanan reported results of three fire-resistance tests on LSF walls. Two wall assemblies, FR2020 and FR2028, were exposed to standard fires, while the furnace time-temperature relationship in the third test, FR2031, was intentionally modified to simulate more "severe" fire exposure. Each wall frame consisted of six cold-formed steel C-shaped studs, the first wall had less height than the others. A single layer of glass-fibre-reinforced gypsum plasterboard lined the steel frames on each side was used. These layers were attached directly to the studs with self-drilling screws. The gypsum board in wall assemblies FR2020 and FR2028 was 16 mm and 12.5 mm thick, respectively, on both sides. Assembly FR2031 had 12.5-mm thick board on the fire-exposed side and 9.5mm board on the ambient side. The structural failures were observed at 72, 44, and 32 minutes in tests FR2020, FR2028, and FR2031, respectively. The researchers noted that walls with low levels of axial load, such as FR2020, might perform better in fire tests than in actual fires because frictional restraints and redistribution of load can enhance the test result [2].

Gerlich used a commercially available computer program, TASEF, to model the heat transfer through LSF walls exposed to fire. The simulations used proprietary, or unspecified, thermal properties of gypsum board. The numerical predictions showed good correlation with temperatures measured in three fire tests. Gerlich used the same basic assumptions formulated by Klippstein to analyse the structural behaviour of load bearing LSF wall. He reported the horizontal deflections calculated from measured temperatures to agree well with measured mid-height deflections. Failure time predictions were most accurate when based on measured temperatures. However, the thermal model was reported to predict greater-than-measured temperature differences across steel stud sections. Therefore, calculated lateral deflections based on TASEF temperatures overestimated the actual mid-height deflections measured in the fire tests. This effect resulted in slightly conservative failure time predictions within 80 to 90% of the test results[2].

Recently, extensive research efforts have been undertaken at the Institute for Research in Construction (IRC), the National Research Council of Canada (NRC), to develop reliable heat transfer numerical models for gypsum board cavity walls. Sultan presented a detailed description of a one-dimensional heat transfer model for non-insulated LSF walls. The model predictions showed promising correlation with temperatures

measured in two fire tests on non-load-bearing wall assemblies. The same experimental data were used to verify similar numerical simulations conducted by Cooper [2].

In 2000 Farid Al fawakhiri and Mohamed A. Sultan presented a paper about comparison of results coming from a numerical simulation and fire tests. Temperature histories across LSF assemblies were simulated numerically by explicit integration of transient heat transfer equations, presenting the lateral deformation histories and predict structural failure times. The model illustrates how different heating regimes in cold formed steel studs cause different structural failure modes. The wall assemblies tested were consisted of a single row of galvanized cold-formed steel studs, protected with two layers of fire-resistant gypsum board (Type X Fire Code C) on each side. All steel studs had a C-shaped cross-section and various types of insulation and resilient channels are often used in LSF wall designs to improve their sound transmission classification (STC) ratings. Three types of insulation materials were used in the tests: glass fibre, rock fibre and dry blown cellulose. Nine resilient channels, attached perpendicular to studs and spaced were used in each test to support the gypsum board on the fire-exposed side. The wall specimens were loaded vertically between two parallel rigid beams and subjected to standard fire on one side. In accordance with CAN/ULC-S101-M89 requirements, nine thermocouples were placed under standard pads on the unexposed side of the wall in each test. These thermocouples were used to detect the heat penetration failure (if any) of the specimens, according to the standard criteria. Using the computer program TRACE (Temperature Rise Across Construction Elements) which employs an explicit integration algorithm (Sultan 1996) to solve one-dimensional transient heat transfer equations for the numerical simulation and it was showing that there was a good agreement between the experimental and the numerical studies [3].

In 2005 Kodur and Sultan conducted 14 full-scale fire resistance tests of load bearing LSF wall panels and found that the insulation type, number of gypsum board layers and stud-spacing had a significant influence on the fire resistance of LSF wall panels. They also found that the use of cavity insulation was detrimental to the fire rating [4].

In 2008, during the 8th Symposium on Building Physics in the Nordic Countries SINTEF (Stiftelsen for industriel logteknisk for skning Foundation for Industrial and Technical Research) [5], published a paper about thermal insulation performance of reflective material layers in well insulated timber frame structures. Presenting the result from a study of the thermal insulation performance of air cavities bounded by thin reflective material layer integrated in well insulated roofs, ceilings, walls and floors using

reflective materials closed air cavities may provide a thermal resistance in roofs and ceilings and walls. As conclusion, the correct way to use a reflective vapour barrier will increase the thermal resistance R-value of closed air cavities integrated in timber frame structures and it is strongly dependent on the heat flow direction. The resistance of a closed air cavity can be equivalent with a conventional thermal insulation layer with a thickness of approximately30 mm for walls and approximately 20 mm for roofs and ceilings. Increasing the air cavity thickness beyond these limits will not increase the thermal resistance of the cavity due to the development of natural convection [5].

In 2012 Ashkan Shahbazian and Yong C Wang [6] published a paper about Direct Strength Method for calculating distortional buckling capacity of cold-formed thin-walled steel columns with uniform and non-uniform elevated temperatures, presented the results of an extensive numerical simulation and analytical study to investigate the applicability of the Direct Strength Method (DSM) to calculating the distortional buckling strength of cold-formed thin-walled (CF-TW) steel members with uniform and non-uniform elevated temperature distributions in the cross-section. For conclusion the uniform temperature applications, the DSM equations in AISI specification are directly applicable, but there is a need for a small modification to improve the accuracy of the method, there is a proposed buckling curve is given. For cross-sections with non-uniform temperature distributions, the DSM concept may still be applied, but a new distortional buckling curve should be used to replace the existing one for ambient temperature calculation with a new expressed in this work. For global buckling, local buckling and distortional buckling (this paper), the same method can be used to calculate the elastic buckling load and the plastic squash load of a column with non-uniform temperature in the cross-section. This method includes the effects of both thermal bowing and shift of the centre of resistance [6].

In 2013 Ashkan Shahbazian, Yong Chang Wang [7] did a work with title of a simplified approach for calculating temperatures in axially loaded cold-formed thin-walled steel studs in wall panel assemblies exposed to fire from one side. This paper proposes a simple method to calculate temperature distributions in the steel section when the panel is exposed to fire from one side. This method calculates the average temperatures in the flanges of the steel section and assumes that the temperature in the web is linear. Simplified approach for calculating temperatures in axially loaded cold-formed thin-walled steel studs in wall panel assemblies exposed to fire from one side, they proposed a method based on simple heat balance analysis for a few nodes representing the key components of the panel, a comparison of the temperature results between the proposed 1-D modelling

and 2-D ABAQUS Finite Element modelling for an extensive set of parametric and sensitivity studies covering different steel section dimensions (width, depth, thickness and lips), different spacing between steel section, number of gypsum layers (1 or 2) and different interior insulation properties. Further assessment of accuracy of the proposed temperature calculation method has been provided by comparing compressive resistance of the steel studs between using temperature profiles produced by 2-D ABAQUS Finite Element simulation and by using the proposed simplified method to check the proposed method in this paper. The results from this work were the following: temperature distribution assumes uniform temperature in each flange and linear temperature distribution in the web between the two flanges. The proposed temperature calculation approach assumed heat transfer in the panel is one dimensional in the thickness direction of the panel. To calculate the weighted average of thermal resistances. This method was easy to implement and gives average flange temperatures that are in very good agreement with ABAQUS 2-dimensional Finite Element heat transfer results. The stud fire resistance times calculated using this proposed design method are in very good agreement with using ABAQUS Finite Element package for both heat transfer and structural analysis [7].

In 2015 Jonathan Vallée [8] presented a master thesis about the reliability of fire barriers using a numerical tools ABAQUS and FDS to reproduce the furnace test, the objectives of this study were to show how the FRR of partitions is affected by leakage. To do this, the FRR obtained from simulations of partitions with localized leakage, distributed leakage, different leakage size and location will be compared to an airtight partition, secondly is to investigate the effect of a reduced thermal insulation on the FRR of partitions. Insulation can be reduced in multiple ways, the scenarios which will be investigated are: localized missing piece of different size of insulation, reduced thickness of insulation, different type of insulation, partition without insulation, hole of different size on the exposed boundary of the partition and hole through the partition. Using methods hand calculations for basic heat transfer through the wall, hand calculations of infiltration and pressure inside the furnace, CFD modelling using the CFD tool FDS and Finite element modelling using ABAQUS to replicate the standard fire furnace tests. The effect on the FRR according to the insulation criterion was examined for the type of insulation or absence of insulation, the reduction of the insulation thickness inside the cavity, breach in the gypsum board exposed in the furnace, breach through the fire barrier and missing piece of insulation inside the cavity. Also, the effect of leakage on the FRR based on the integrity criterion will be investigated assuming that the barrier leaks before it is submitted to the

standard fire. No experiments were done during this study. The conclusions of this work were for partition without deficiencies or alteration, stone wool insulation provided a FRR higher compared to similar partition insulated with glass Fibre wool and uninsulated partition, the results showed also that using stone wool insulation inside the cavity could help improving the FRR, based on the insulation criterion. This study showed a method to simulate fire resistance test with the help of numerical tools. This could be very useful, especially when considering the high cost of testing samples in furnaces. Still, much work needs to be done in order to accurately model a fire resistance test [8].

At the Polytechnic Institute of Braganca (IPB) several experimental and numerical works were done for the aim of developing accurate numerical models based on the thermal analysis with fluid structure interaction [9] and to validate the numerical models with tests performed by other researchers [10]. An analysis of the fire behaviour of a simple light weight steel walls LSF using the simplified one-dimensional heat flow [11], presenting a sequential numerical model to study the fire resistance of LSF walls made with composite panels under load bearing condition with numerical models [12], and experimental fire tests were developed to define the fire resistance of the partition walls, and compare the behaviour of composite plates with the traditional solution using gypsum protection plates. These tests were simulated with three-dimensional (3D) finite-element models using ANSYS applying the hybrid solution method FEM-H for nonlinear thermal analysis. The numerical results agree well with the experimental results, for all the measured quantities, including the maximum and average temperature for the unexposed surface. The maximum difference for the fire resistance is below 12%, for most of the specimens [13].

In 2020 Khetata et al published an article with seven small-scale specimens that were tested to define the fire resistance of non-load bearing light steel frame walls made with different materials. All tests were validated using two-dimensional numerical models, based on the finite-element method, the finite-volume method and hybrid finite-element method. The numerical results presented a good agreement with the fire tests [14].

Anthony Deloge Ariyanayagam and Mahen Mahendran investigated the impact of utilizing low strength steel studs, noggins and cavity insulation. Results obtained showed that the use of cavity insulation significantly minimized the fire resistance level (FRL) of load bearing walls while the use of noggins increased the FRL of load bearing walls due to reduced lateral deflections of walls. Structural limited element models of tested LSF wall studs were developed and approved utilizing the fire test results, which was taken after by

a numerical parametric study to further assess impacts of utilizing studs made of diverse review steels on the fire execution of LSF walls [15].

Chapter 3: Fire resistance of LSF walls

The Light-weight Steel Frame constructions showed up within the end of the XX century, and have as principal benefits: high-load bearing capacity, the weight of the structure and a wide extend of possibilities and arrangements. The definition of LSF, given by [16], could be a composite of a steel mesh supporting all loads, with plate-like dividers covering the ranges and shaping the construction. They are made of sandwich sort and the metal structure encompasses a plate on each side as security layer. Walls can or don't withstand loads, and the material commonly utilized for the plan of the assurance layer is gypsum.

Lightweight Steel Frame Walls (LSF) are broadly utilized within the construction industry, due to their solidness higher strength-to-weight proportion and progressed heat resistance. The LSF wall framework comprises of cold shaped steel studs, fire security boards and separator in different layouts. Fire resistance is a critical design parameter in LSF wall construction, since the thin-walled cold-formed steel studs warm-up rapidly and lose their quality and dur ability. Subsequently, the studs are secured by plasterboards to delay the warm exchange through them and progress the fire resistance of LSF walls. Different layers of fire evaluated gypsum plasterboards or other comparative sheets with or without depression separator are commonly utilized for detached fire security of LSF walls. Fire resistance of LSF walls is measured in terms of Fire Resistance Level (FRL), which is, the time period during which the components stand up to the fire under three criteria, are Load-bearing capacity, Integrity and Insulation [17].

3.1. Fire resistance criteria

Fire resistance criteria are the properties that describe the ability of a specimen of system construction to prevent the spread of flame or smoke in a fully developed fire, and maintain structural stability of the tested specimen. These parameters are Load-bearing capacity, Integrity and Insulation.

3.1.1. Load bearing capacity

The load bearing resistance (R) is the ability to support the structural loading without collapsing or suffering excessive deformations. When ignoring the membrane action, three different failure modes are relevant: flexural failure, longitudinal shear failure and vertical shear.

The international standard ISO 834 [18],specifies performance criteria for flexural elements for the maximum deflection D (mm) and the maximum deflection rate dD/dt (mm/min), as presented below.

$$D = \frac{L^2}{400 \cdot d} \quad (1)$$

$$\frac{dD}{dt} = \frac{L^2}{9000 \cdot d} \quad (2)$$

In the last equations, L is the clear span of the structural element (mm), and d is the distance from the extreme fibre of the cold design compression zone to the extreme fibre of the cold design tensile zone of the structural section (mm)[19].

3.1.2. Integrity

The integrity criterion (E) is the capacity to withstand fire in one side and resist penetration of hot gases and flames. The assessment should be made on the basis of measuring cracks or openings in excess of given dimensions, or the ignition of a cotton pad, or sustained flaming on the unexposed side. For cast in situ composite slabs, the integrity criterion is normally satisfied provided that the joints are adequately sealed [19].

3.1.3. Insulation (I)

The thermal insulation criterion (I) is the ability to withstand fire in one side and prevent excessive transmission of heat. The assessment shall be made on the basis of the average temperature rise on the unexposed surface limited to 140 °C above the initial average temperature, or; on the basis of the maximum temperature rise at any point on the unexposed surface limited to 180 °C above the initial average temperature [19].

3.2. Standards to be followed

The standards used to obtain the fire resistance of loading bearing LSF walls are the EN 1363-1 (Fire Resistance Tests - General Requirements) and Eurocode 3 (EN 1993-1-2 - Design of Steel Structures - General Rules: Structural Fire Design).

3.2.1. EN 1363-1

The EN 1363-1 sets up the common standards for deciding the fire resistance of different components of development, when subjected to standard fire exposure conditions [19]. A specially designed furnace is required to subject the test specimen to the test conditions. The system to control the temperature of the furnace, the equipment to control and monitor the pressure of the hot gasses inside the furnace, the frame in which the element can be inserted and submitted to suitable heating, pressure and support conditions. The arrangement for loading and limitation of the test specimen should be suitable, including control and observing of the load equipment for measuring temperature in the furnace and within the test specimen. For some cases, the system for measuring the deflection of the test specimen is required. Moreover, in some cases, particular devices are required to evaluate the integrity and for setting up compliance with the performance criteria. For very special cases, the equipment for measuring the oxygen concentration of furnace gases is too required. This standard for testing moreover indicates the design and resistances about systems, including some draws about the sensors, such as the disk thermocouples and plate thermocouples

The performance criteria "insulation" shall automatically be assumed not to be satisfied when the "integrity" measure ceases to be satisfied. The integrity criteria (E), in this case, concern about the time of flame or smoke pass through the unexposed side by some crack. It’s important clarify that the main performance criteria given by this standard is the load bearing criteria or stability. The load bearing resistance (R) is the capacity to support its test load without passing specified criteria with respect to the extent of deflection or rate of deflection.

3.2.2. EN 1993-1-2

The Eurocode 3 (EN 1993-1-2) applies to the design of steel buildings. It complies with the principles and necessities for the safety and serviceability of structures. The basis of their design and edification are given in EN 1990 –Basis of basic design. The EN 1993-1-2 deals specifically with the design of steel structures for the accidental condition in fire [20].

Walls made with LSF have a steel structure. The load-bearing function of a steel member should be expected to be maintained after a time t in a given fire, in the event that the condition in the equation (4.1) is satisfied. $E_{fi,d}$ is the design impact of actions for the fire design situation, concurring to EN 1991-1-2 and $R_{fi,d,t}$ is the corresponding fire design resistance of the steel member at time t.

$$E_{fi,d} \leq R_{fi,d,t} \qquad (3)$$

For class 4 cross-sectional elements other than tensile elements, it can be assumed that this relation is satisfied, if at time t, the temperature of the steel at all the sections is not above a critical temperature, recommended as $\theta_{crit} = 350^{\circ}C$. This criterion can be too conservative and dangerous for specific cases, because this simple method is independent of the load ratio. This criterion will be used to assess the stability of the wall, just in case of loading conditions must be applied.

3.2.3. Standard Fire Curves ISO 834

The standard models of fire are approaches of the characteristic fire bend and are autonomous of space and fire stack thickness. This bends for the most part approach the "flashover" and the nonstop combustion, that's the foremost basic periods of fire within the auxiliary and thermal studies. The Eurocode 1 managing with activities on structures uncovered to fire [18] presents three nominal bends of fire: the standard bend, too called ISO834, the outside components curve and the bend of fire caused by hydrocarbons

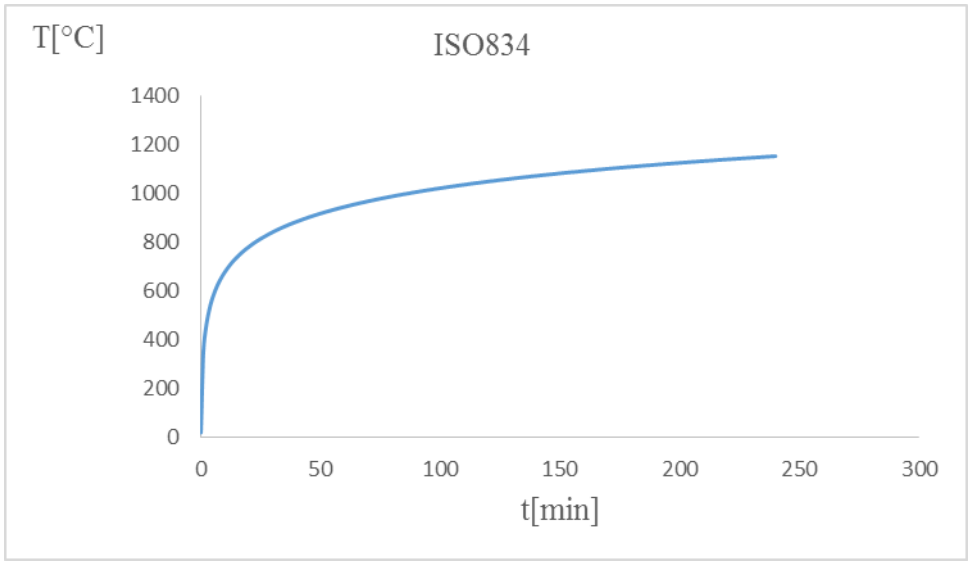

Figure 1: ISO 834 Standard Curve

Chapter 4: Heat transfer

Thermal transmittance of the building envelope influence to a great extent the overall thermal performance and energy efficiency of the building. That is why, it is essential to accurately determine the thermal transmittance U-value of the main building envelope elements. Studies that investigates the fire resistance of walls require determination of later heat exchange with adjunct construction.

Heat energy can be exchanged from one body to the other or from one area in a body to another. Study of the procedures and strategies embraced to exchange heat energy is known as 'Heat Transfer'. To encourage heat exchange between 2 bodies there should be a temperature contrast between them. This implies that these bodies must be 2 distinctive temperatures, one higher than the other to permit heat to flow from one body to the other. In fact, heat is characterized as energy exchanged by virtue of a temperature contrast. This implies that no heat exchange happens between 2 bodies which are at the same temperature. At the same time, it is exceptionally imperative to note that heat streams from regions of higher temperature to locales of lower temperature. It is standard to refer to diverse sorts of heat exchange mechanisms as modes. The fundamental modes of heat exchanges are conduction, radiation, and convection [21].

4.1. Radiation

Radiation, or more accurately thermal radiation, is electromagnetic radiation transmitted by a body by ideals of its temperature and at the cost of its inside energy. In this way thermal radiation is of the same nature as visible light, x beams, and radio waves, the contrast between them being in their wavelengths and the source of era. The eye is delicate to electromagnetic radiation within the locale from 0.39 to 0.78 ~ tm; this is often distinguished as the unmistakable locale of the range. Radio waves have a wavelength of 1 x 10^{3} to 2 x 101 ~ tm, and x beams have wavelengths of 1 × 10^{-5} to 2 x 10^{-2} ktm, whereas the bulk of warm radiation happens in beams from approximately 0.1 to l00 ktm. All warmed solids and fluids, as well as a few gasses, emanate warm radiation. The exchange of vitality by conduction requires the nearness of a material medium, whereas radiation

does not. In reality, radiation exchange happens most productively in a vacuum. On the plainly visible level, the calculation of warm radiation is based on the Stefan Boltzmann law, which relates the energy flux transmitted by an perfect radiator (or blackbody) to the fourth power of the absolute temperature [21].

4.2. Convection

Convection, in some cases distinguished as an isolated mode of heat exchange, relates to the transfer of heat from a bounding surface to a liquid in movement, or to the heat exchange over a stream plane within the insides of the streaming liquid. In case the liquid movement is actuated by a pump, a blower, a fan, or a few comparable gadgets, the method is called constrained convection. On the off chance that the liquid movement occurs as a result of the thickness distinction delivered by the temperature distinction, the method is called free or characteristic convection. Detailed assessment of the heat exchange prepare in these cases uncovers that, in spite of the fact that the bulk movement of the liquid gives rise to heat exchange, the essential heat exchange component is conduction, i.e., the energy exchange is within the form of heat exchange by conduction inside the moving liquid. More particularly, it isn't heat that's being convicted but inside energy. In any case, there are convection forms for which there’s, in expansion, idle heat exchange. This inactive warm trade is for the most part related with a stage alter between the liquid and vapor states of the liquid. Two uncommon cases are bubbling and condensation [21].

4.3. Conduction

Conduction is the exchange of heat from one portion of a body at a better temperature to another part of the same body at a lower temperature, or from one body at a better temperature to another body in physical contact with it at a lower temperature. The conduction handle takes place at the atomic level and includes the exchange of energy from the more energetic molecules to those with a lower energy level. This may be effort lessly visualized inside gasses, where we note that the normal active energy of atoms within the higher-temperature locales is greater than that of those within the lower-temperature locales. The more energetic molecules, being in steady and irregular movement, occasionally collide with particles of a lower energy level and transfer energy and force. In this way there's a persistent transport of vitality from the high-temperature locales to those of lower temperature. In fluids the molecules are more closely divided than in gasses, but the atomic energy exchange proceed [21].

Chapter 5: Numerical simulation

Special numerical tasks aimed to develop an accurate model to predict fire resistance and the validation of the 3D finite element models. This chapter presents the numerical validation of the experimental tests

5.1. ANSYS Multiphysics Software

5.1.1. General

ANSYS is a general commercial finite element analysis package which was released in the decade of 1970. Nowadays, this tool is largely used in engineering simulation to solve involving thermal problems, structural and fluid analysis.

The ANSYS Mechanical APDL 18.2 [22] is a powerful software which use the FEM to find solutions to the linear and nonlinear problems in either steady-state or transient regime, comprising 2-D or 3-D geometries. Several types of finite elements were used in this computer program and permitted the introduction of commands through graphical user interface and command prompt as well.

5.1.2. Element types

Two different types of finite elements from the ANSYS library are used, namely SHELL131 and SOLID70.

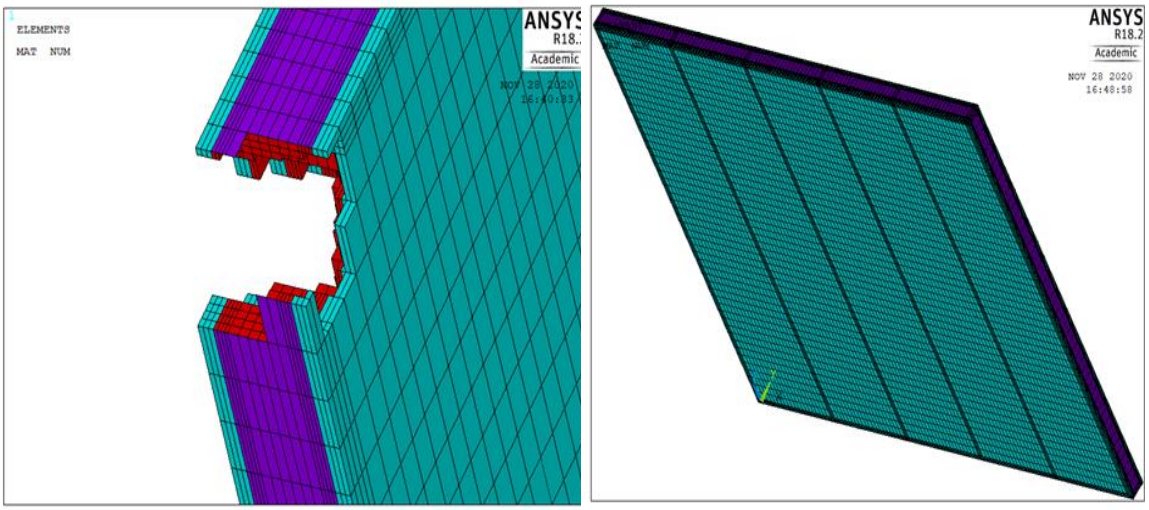

Figure 2: Finite element mesh used from model in solution method

The shell 131 has four nodes with up to 32 degrees of freedom (temperature) per node, depending on the number of layers (one layer). This element presents linear interpolation functions within the plane of the element, utilizing full Gauss integration method 2x2 and linear interpolation functions through the layer thickness (three Gauss points). The bottom temperature of the element is utilized shell element nodes is accepted to be equal to the temperature of solid element nodes utilizing the function “Paint (TBOT → TEMP)”, when both nodes are coincident. The shell131 generates temperatures that can be passed to structural shell elements in order to model thermal bending. The shell was used to model the steel frame (track and Stud). Figure 3 presents the geometry, node locations and the global and local coordinates systems of the SHELL131 element.

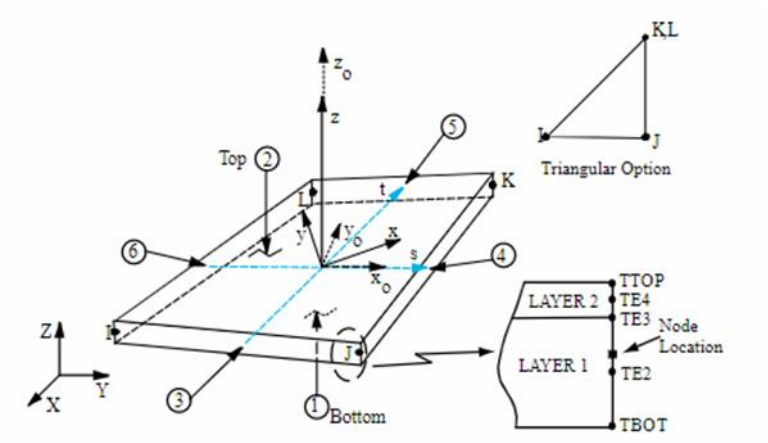

Figure 3: The SHELL131 finite element

The SOLID70 element presents eight nodes with a single degree of freedom (temperature) at each node. Linear interpolation functions are used for this element and the full Gauss integration method 2x2x2 is also applied. The element also can compensate for mass transport heat flow from a constant velocity field. The SOLID70 was used to model the gypsum and glass fibre Figure 4 illustrates the SOLID70 geometry in global and local coordinate systems as well as the node locations.

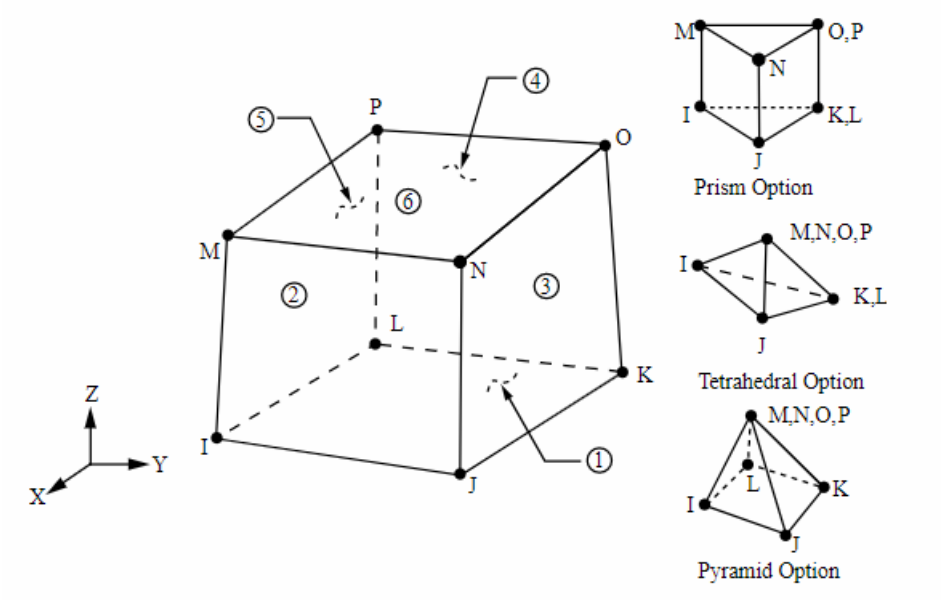

Figure 4: The SOLID70 finite element

5.2. Material properties

The thermal properties are decisive to simulate the performance of the load bearing wall. The thermal properties are temperature dependent for all the materials involved.

5.2.1. Thermal property of Steel

Steel presents typical evolution for the specific heat with a maximum value that accounts to the allotropic transformation. The thermal conductivity depends on temperature and specific mass is considered constant. The thermal property was used by [20].

- Specific heat

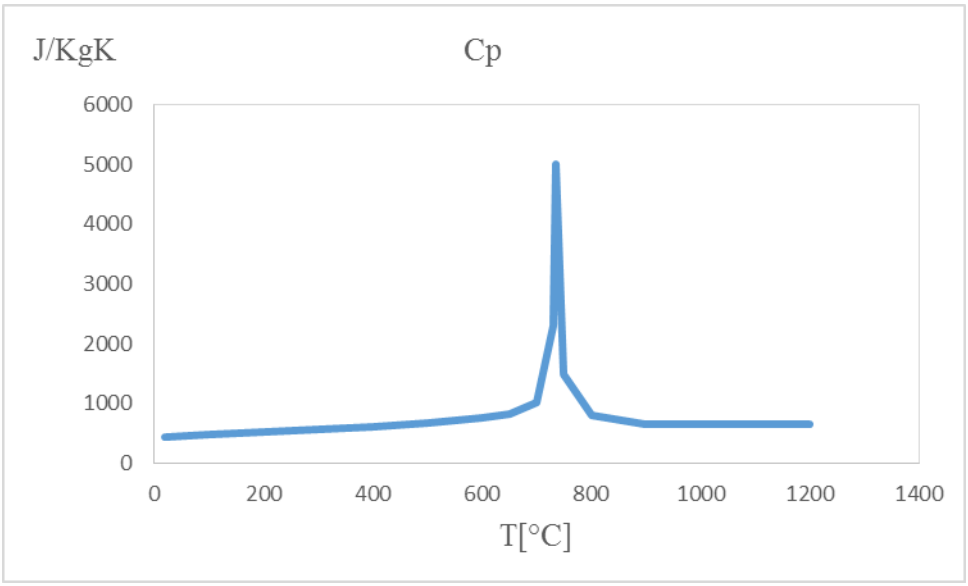

Figure 5: Specific heat of steel

- Conductivity

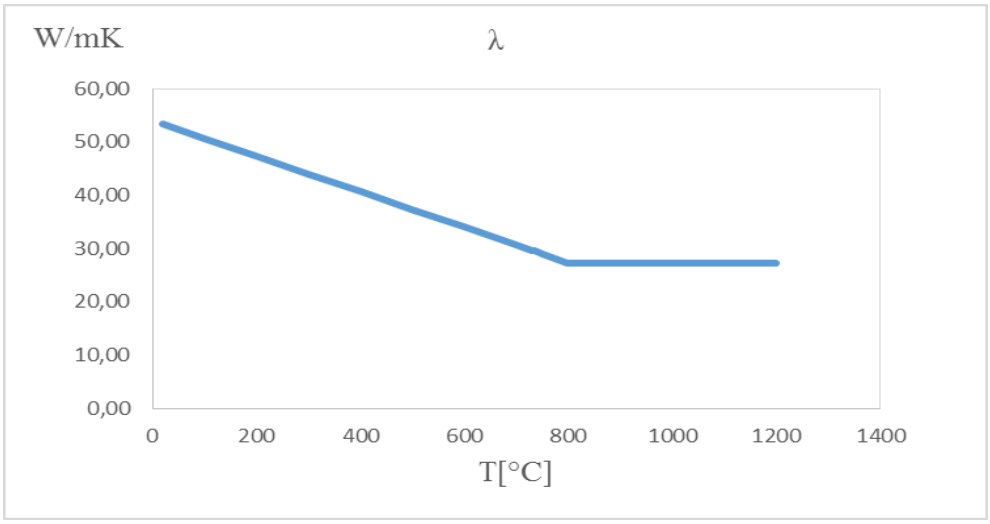

Figure 6: Conductivity of steel

- Specific mass

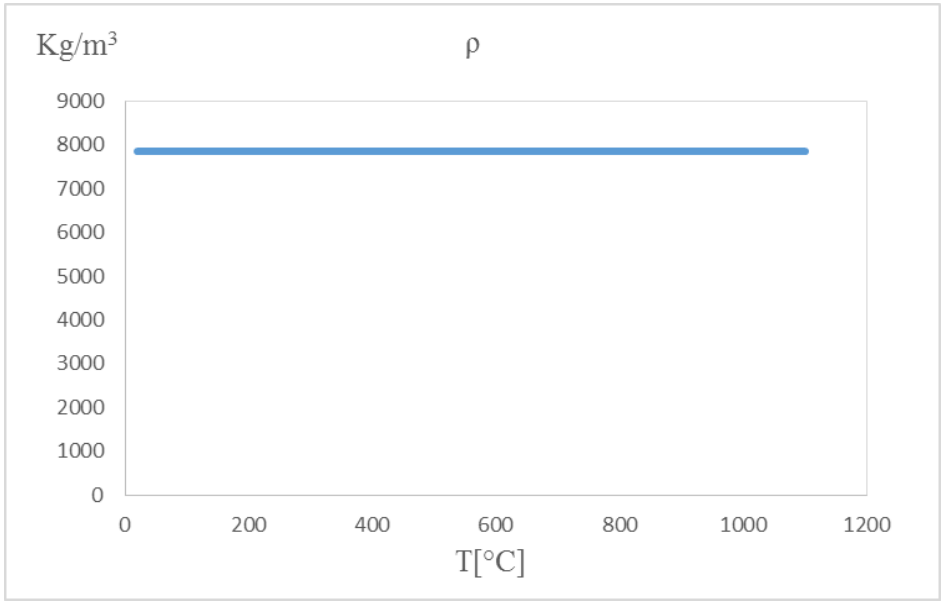

Figure 7: Specific mass of steel

- Emissivity

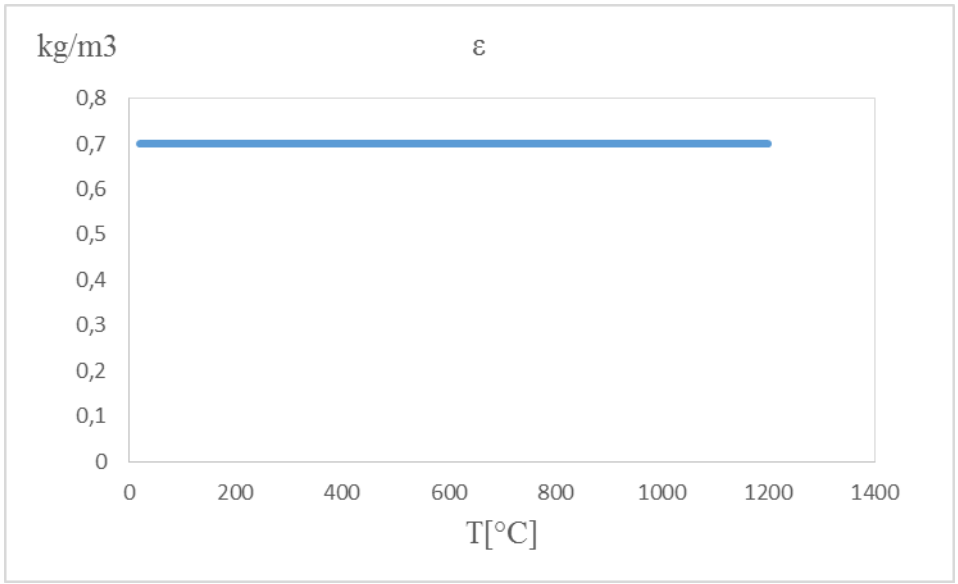

Figure 8: Emissivity of steel

5.2.2. Thermal property of Gypsum

The thermal properties of Gypsum considered in this investigation for the specific heat, thermal conductivity and for the specific mass. This thermal property was used by [1].

- Specific heat

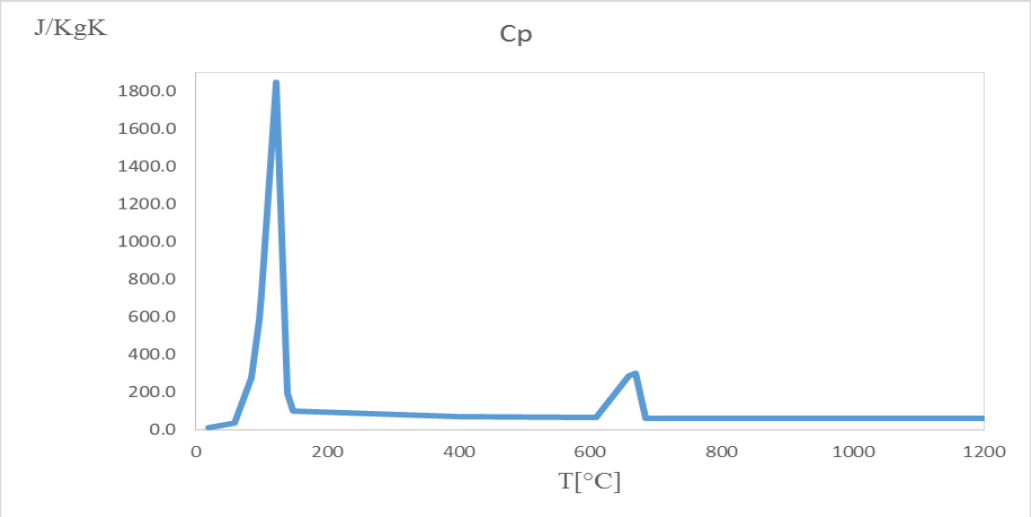

Figure 9: specific heat of gypsum

- Conductivity

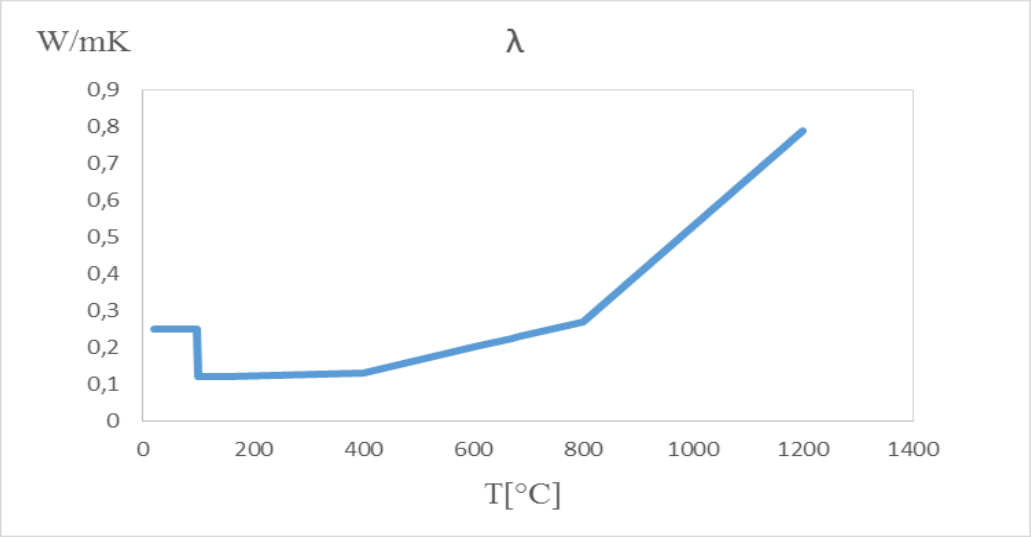

Figure 10: Conductivity of gypsum

- Specific mass Kg/m^3

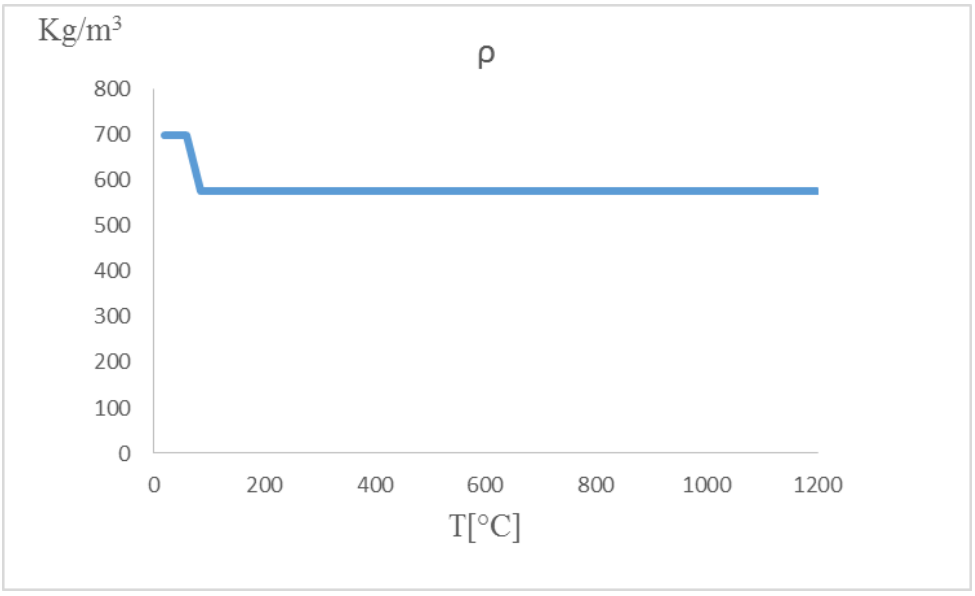

Figure 11: Specific mass of gypsum

- Emissivity

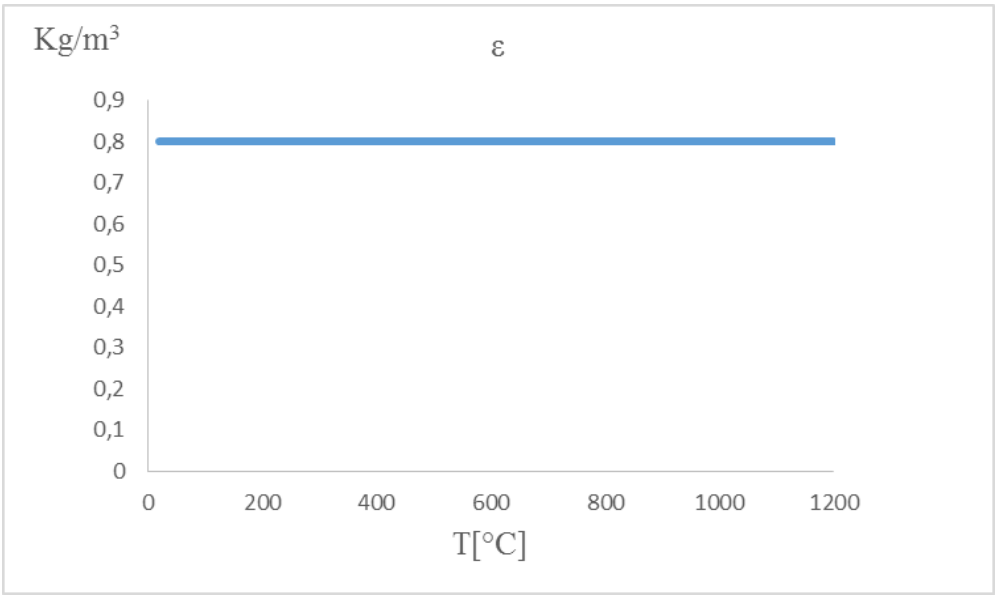

Figure 12: Emissivity of gypsum

5.2.3. Thermal property of Glass fibre

The thermal properties of the Glass fibre depend on the fabrication process. During the production process the fibres are pressed to achieve different densities, being the heaviest ones produced as boards and the lightest as mats. The fibre itself starts melting around 1200°C. This thermal property was used by [15].

- Specific heat

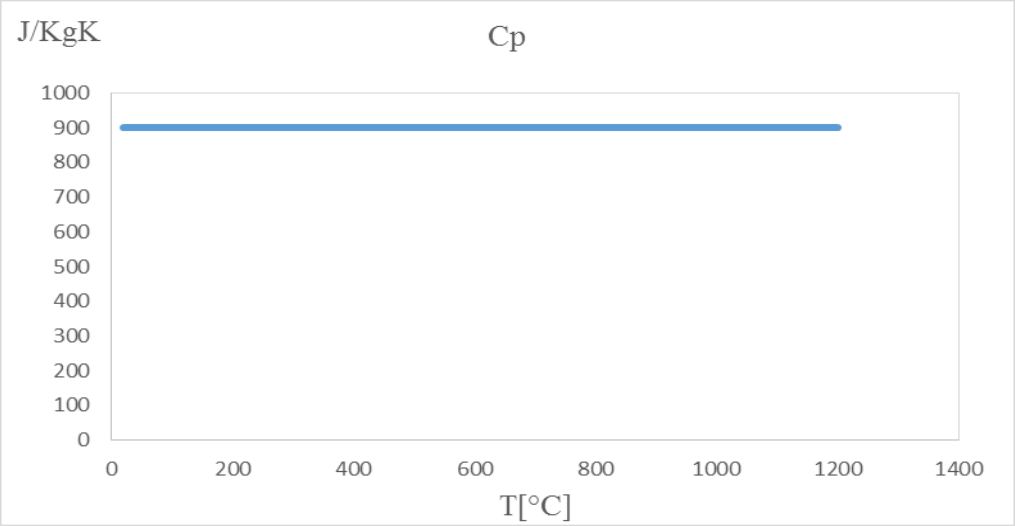

Figure 13: Specific heat of glass fibre

- Conductivity

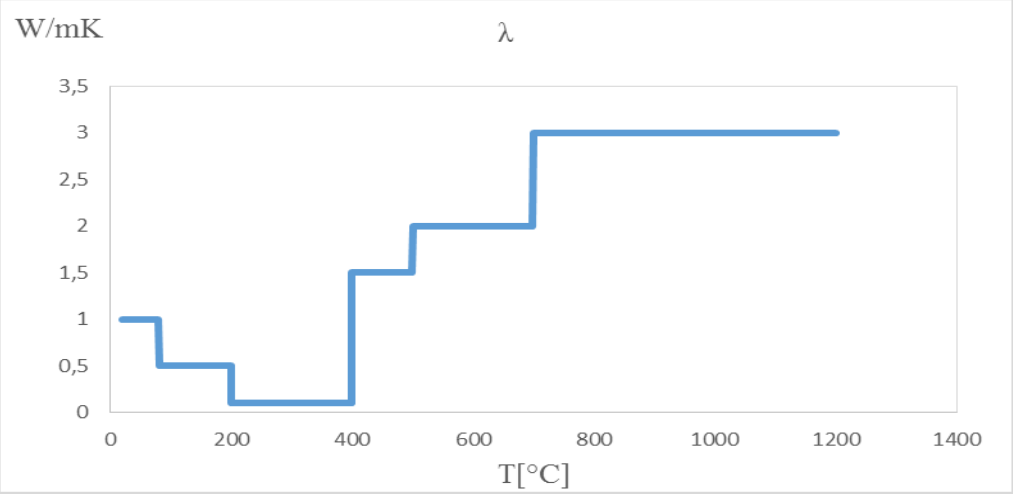

Figure 14: Conductivity of glass fibre

- Specific mass

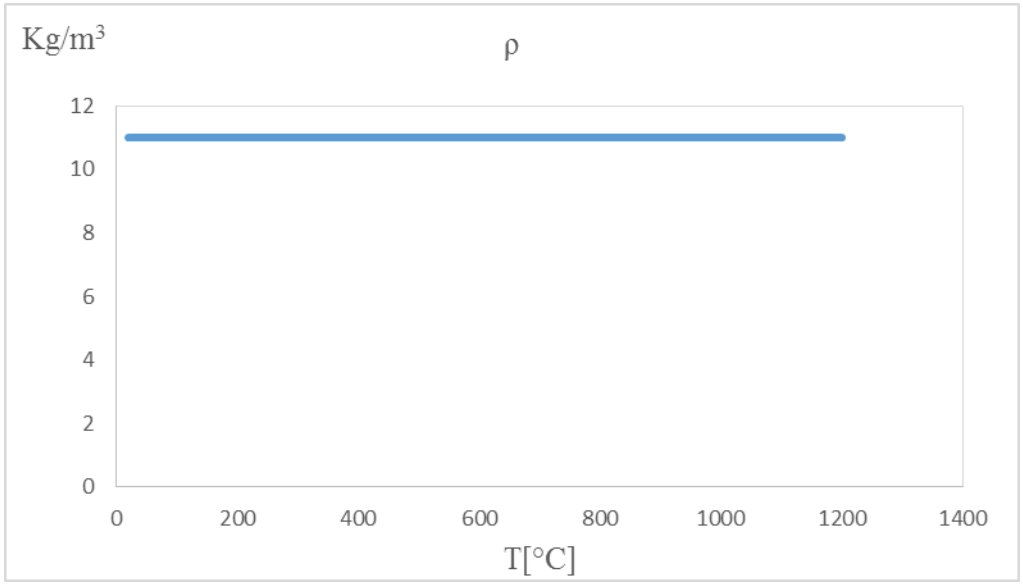

Figure 15: Specific mass of glass fibre

- Emissivity

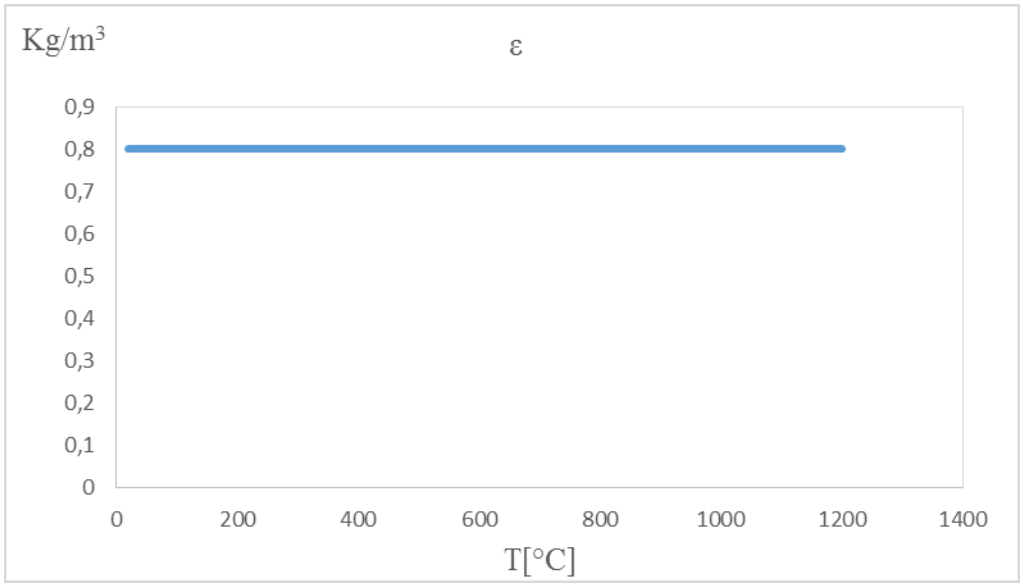

Figure 16: Emissivity of glass fibre

5.3. Boundary conditions

One side of the wall was submitted to fire and the other side is accepted to remain in contact with room temperature. Assuming warm exchange by radiation (emissivity of fire ε = 1) and convection (convection coefficient α = 25W/m^{2}K) in the fire side and heat exchange by convection (convection coefficient α = 9W/m^{2}K) in the unexposed side. The gas temperature in the fire side follows the standard ISO834 [18]. The room temperature of the unexposed side is assumed equal to the beginning temperature (T = 20°C), during all the simulation time.

With regard to the radiation options, a value of 5.67E-8 is characterized for the Stefan-Boltzmann constant, and a value of 273.15 is set for the temperature difference between absolute zero and zero of the dynamic temperature scale (temperature offset). Thereafter, the space node following the standard fire curve is relegated to the enclosure. Finally, the radiation boundary conditions are applied on the elements of the fire exposed surface, following the temperature of the enclosure already characterized.

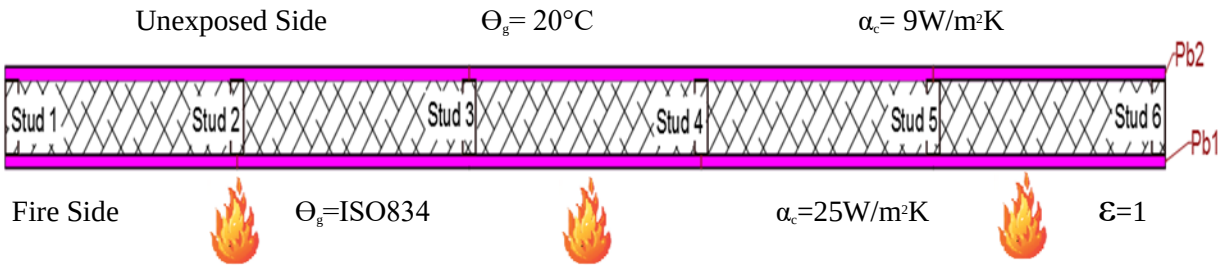

Figure 17: Boundary conditions

5.4. Numerical validation analysis

5.4.1. Configuration of the test to be validated

The test specimen geometry was taken from the journal paper of Anthony Deloge Ariyanayagam, Mahen Mahendran [15]. The LSF wall (3mX3m) was a single wall with six studs G300 type C 92-35-15-1.15, spaced by 600 mm, lined with one plasterboard layer with 16 mm of thickness type X from both sides. The cavity was fulfilled by a glass fiber insulation with density of 11 Kg/m^3, the figure below demonstrates the model in details.

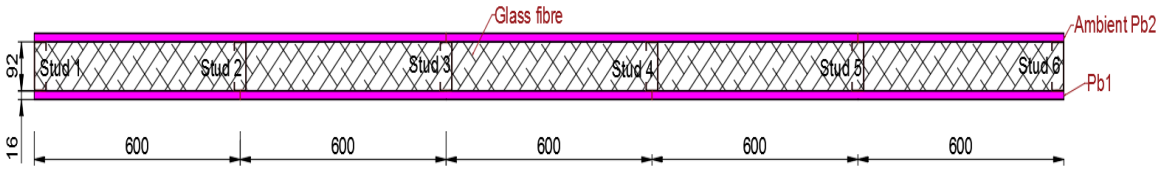

Figure 18: LSF wall dimensions

The figures down present the average temperature results obtained from the numerical simulation three dimensions on different locations of the non-load bearing wall, the data were collected at selected nodes throughout the finite element mesh.

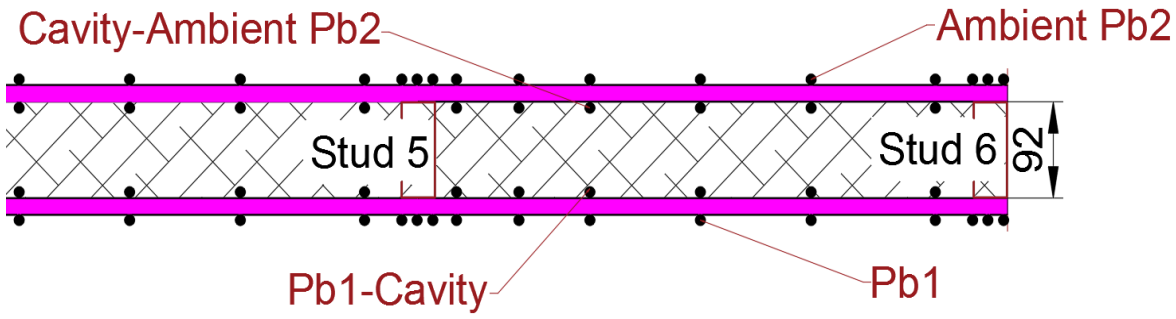

Figure 19: Nodal temperatures distribution used the average temperatures

The figure 19 present the temperature values from the test and simulation on specific same minutes of different regions on the model:

- PB1 refers to Plasterboard layer1,
- PB1-CAVITY refers to the bottom interface between the insulated cavity and the first protection layer,
- Cavity-Ambient_PB2 refers to top interface between the full cavity and the unexposed gypsum plate,
- Ambient _PB2 refers to unexposed surface.

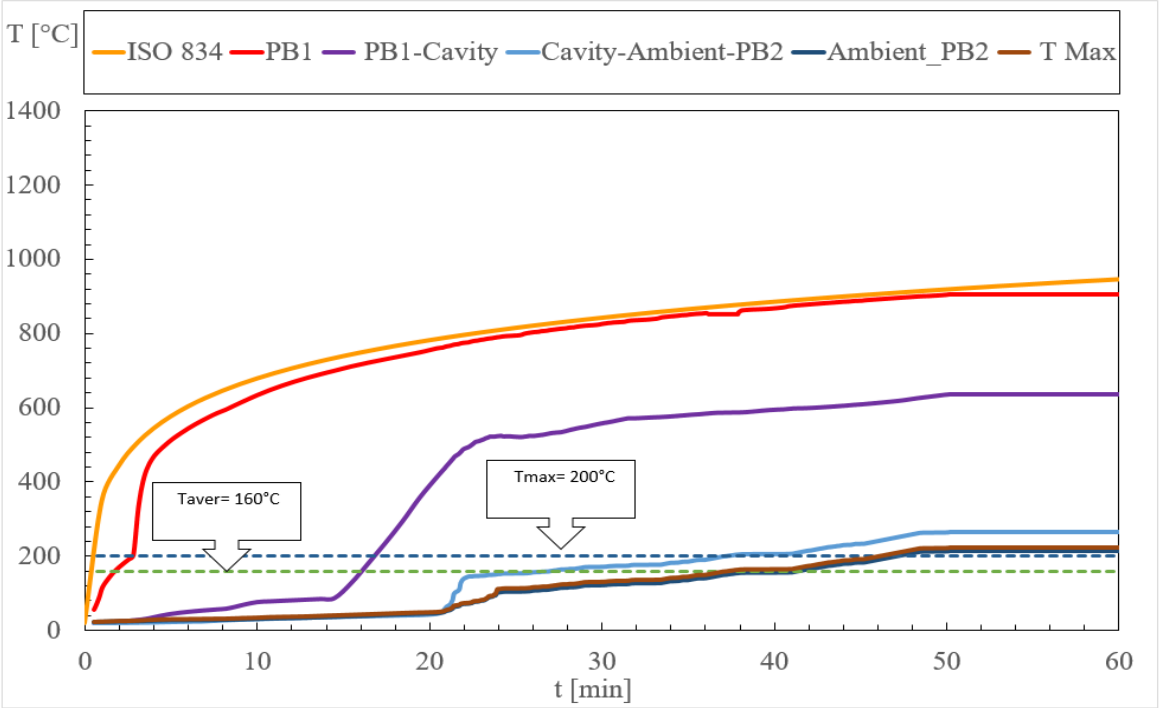

Figure 20: Average numerical results of test 4

Using perfect contact and sometime the experimental stood can not allow for perfect contact.

The moisture of the gypsum is different from the material property.

The maximum and average temperature of the unexposed side was determined using nodal temperature applied on the unexposed side, the failure time for the average temperature of the unexposed surface was at the minute 41, while the for the maximum temperature reached 200 °C, at the simulation time of 45 minutes.

This figure present the mid-point temperature on the haut flange and the cold flange for the studs 2, 3, 4 and 5

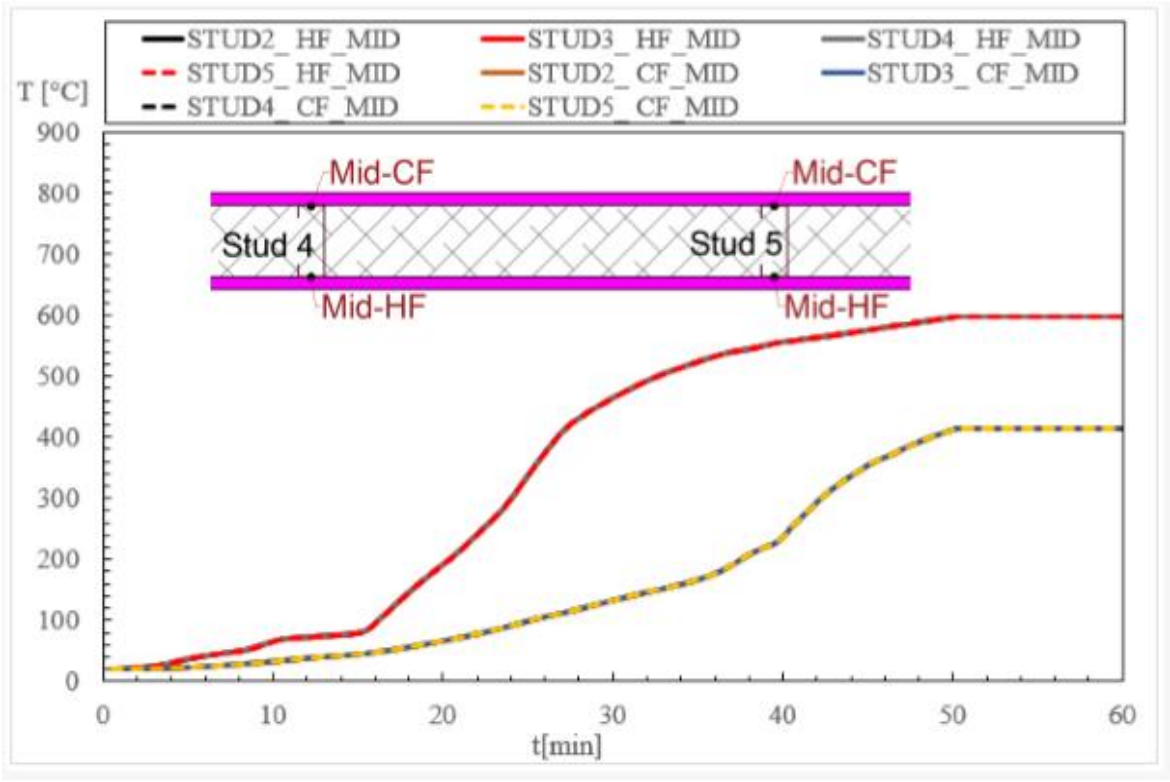

Figure 21: Average temperature on the mid cold and hot flanges

This figure present the point temperature on the haut flange and the cold flange for the studs 3 and 4

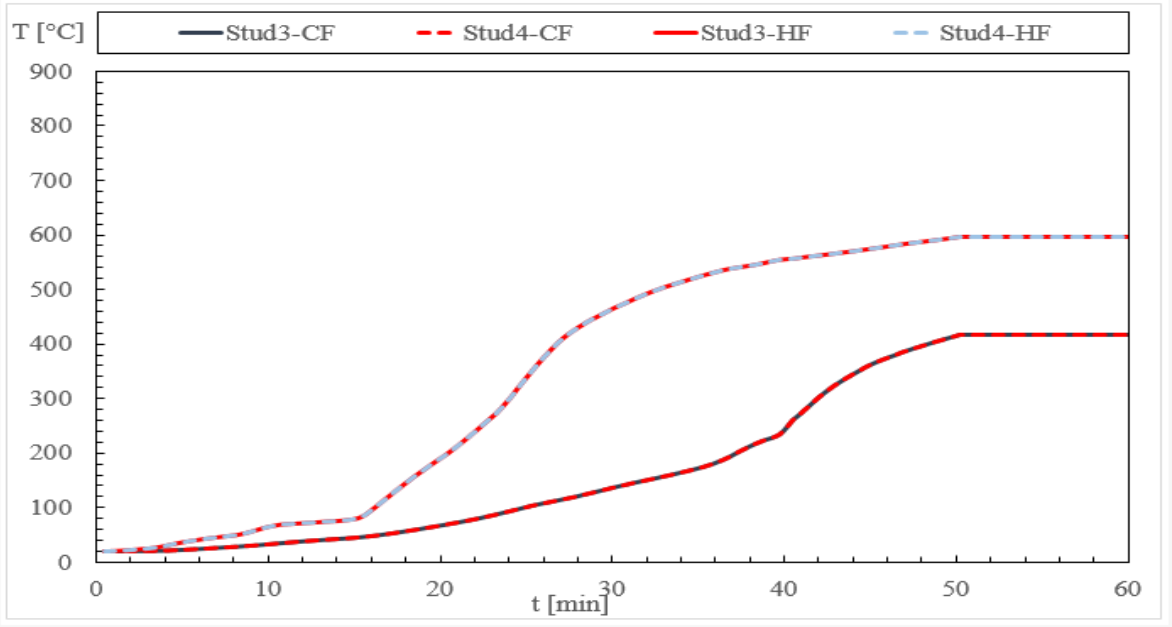

Figure 22: Average temperature on the cold and hot flanges

5.4.2. Comparison between numerical and experimental results

This graph illustrates the both average results from the experimental test done by[15] and there numerical validation developed on the Ansys software.

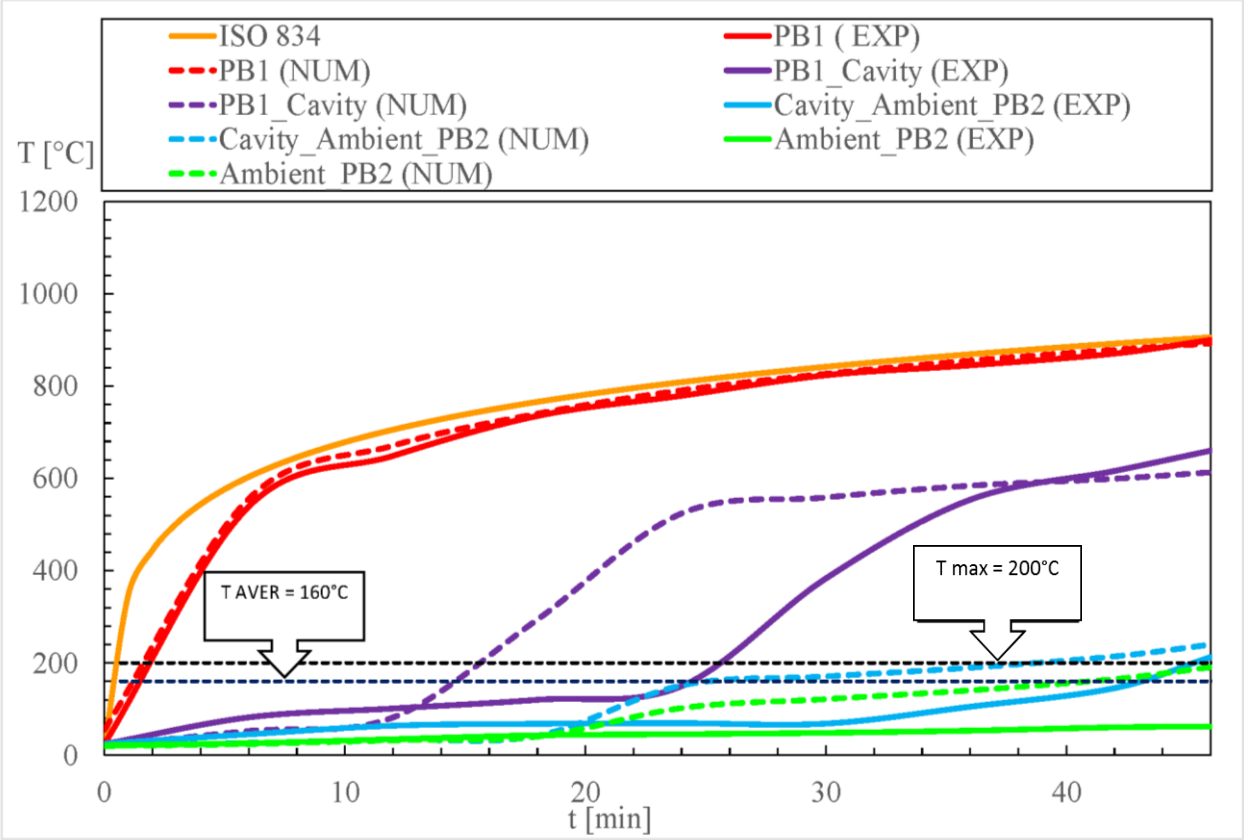

Figure 23: Numerical and experimental results for Test 4

It is noted that the numerical results are higher than the experimental ones, the tables below present the temperature values from the test and simulation on specific same minutes

Table 1: Numerical Simulation results

Numerical Simulation					
t[s]	t[min]	PB1[°C]	PB1_CAVITY[°C]	Cavity_Ambient_PB2[°C]	Ambient_PB2[°C]
240	4	476.8	37.2	25.25	22.01
480	8	595.51	59	28.03	27.1
960	16	721.1	197.07	40.24	38.5
1200	20	760.12	413.3	45.5	44
2160	36	855.23	584.01	189.56	140.45
2760	46	892.35	613.01	239.66	190.55

Table 2: Experimental results

Experimental					
t[s]	t[min]	PB1[°C]	PB1_CAVITY[°C]	Cavity_Ambient_PB2[°C]	Ambient_PB2[°C]
240	4	456.07	58.89	25.07	22.41
480	8	554.7	86.12	55.01	26.1
960	16	685.04	115.01	66.38	41.1
1200	20	740.02	124.8	68.37	43.13
2160	36	844.9	553.62	105	53.15
2760	46	900	654.01	212.54	62.12

$$RMS = \sqrt{\frac{1}{n} * \sum_{i=1}^{n} \left(\frac{\text{T numerical} - \text{T experimental}}{\text{T experimental}} \right)^2} \qquad (6)$$

Table3: Root mean square comparison

t[s]	t[min]	RMS PB1 (num)/PB1(exp)	RMS PB1_CAVITY(num)/ PB1_CAVITY(exp)	RMS Cavity_Ambient_PB2(num)/ Cavity_Ambient_PB2(exp)	RMS Ambient_PB2 (num)/ Ambient_PB2 (exp)
240	4	0.043	1.007	0.442	1.3
480	8				
960	16				
1200	20				
2160	36				
2760	46				

Used the RMS equation to compare the numerical and experimental average temperatures results demonstrate great agreement and small error

The Table 4 demonstrates the comparison between the experimental and numerical results presented on the previous tables, calculated by the relative errors equation

$$RE\ [\%] = \left(T_{experimental} - T_{simulated} / T_{experimental} \right) X\ 100 \quad (7)$$

A comparison of the fire resistance by the average temperature between the fire test and numerical model is presented on the Table 4.

Table 4: Relative error T_{max} and T_{aver}

Fire resistence TEST T_{aver} (min)	Fire resistence SIMULATION T_{aver} (min)	Relative Error %
47	41	12.7

The comparison of the experimental and numerical results showed a good agreement

5.5. Parametric analysis

As the model was predicting reasonably well with the experimental results, we settled to analyze the effect of the cavity thickness, stud dimensions and the number of protection layers. The fire resistance was determined for most of the cases, taking into consideration the insulation criterion (I). Using numerical 2D solution model.

5.5.1. Model number 1

In this cross section we decided to keep the same configuration of the LSF wall (6 Studs type C 92-35-15-1.15), complete cavity fulfilled by the glass fibre insulation.

The only difference of the validated test model is the number of protection layers which are 2 gypsum boards of 16 mm thickness. (See the figure below).

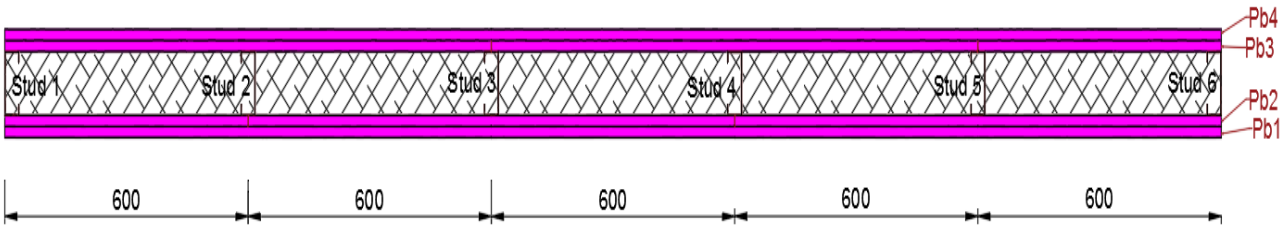

Figure 24: Cavity insulated and 2 plasterboard lined LSF wall

- **Results of the model number 1**

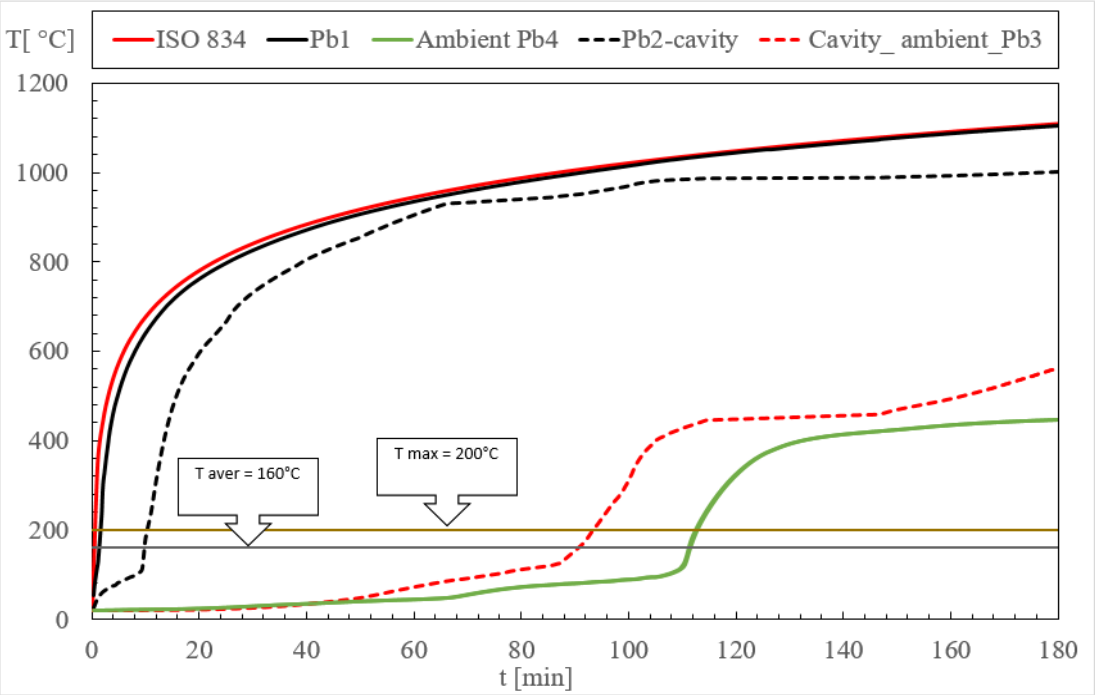

Figure 25: Temperature profiles represent the average values in (fire side, cavity, and unexposed side)

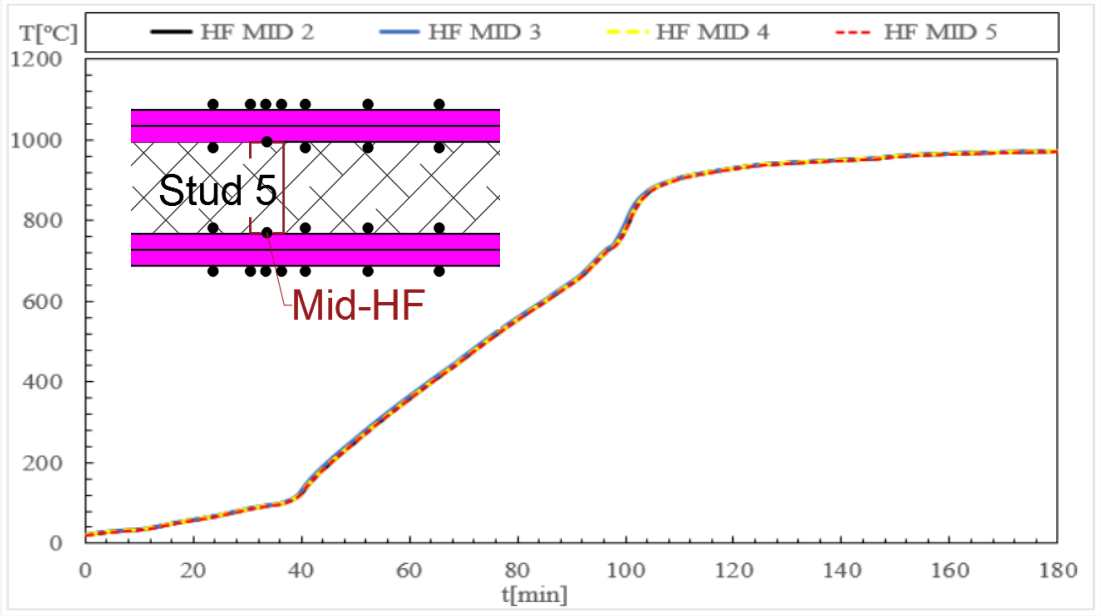

Figure 26: Numerical results for the parametric analysis on mid hot flanges

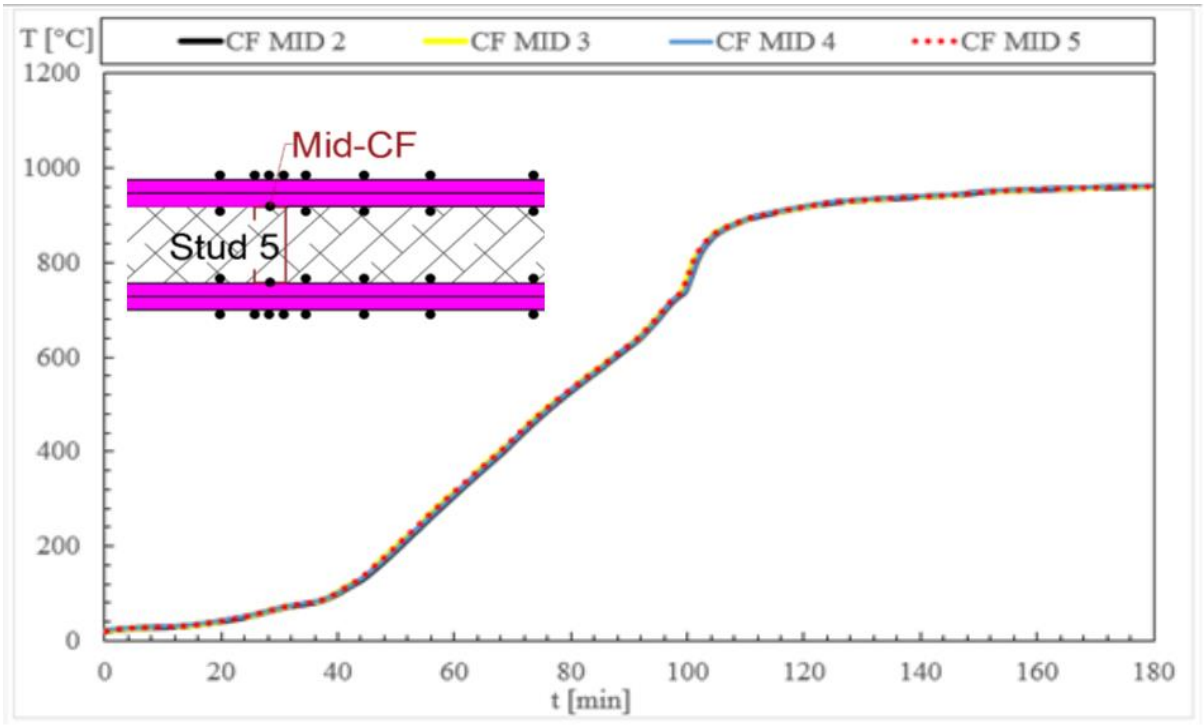

Figure 27: Numerical results for the parametric analysis on mid cold flanges

The numerical solution results of the LSF wall under fire ISO 834 standard condition are demonstrated in the Figure 25. The fire resistance was determined by the average temperature (160 C°), the failure time of this model was at the minute 111, while the criteria for the maximum temperature was reached after 112 minutes. From this simulation results we can note that the addition of one Gypsum layer improved the fire resistance.

5.5.2. Model number 2

In this cross section we want to keep the main configuration of the LSF wall (6 Studs type C 150-50-10-1), complete cavity fulfilled by the glass fibre insulation.

The only difference of the validated test model is the dimension of the stud and the cavity thickness. (See the figure below).

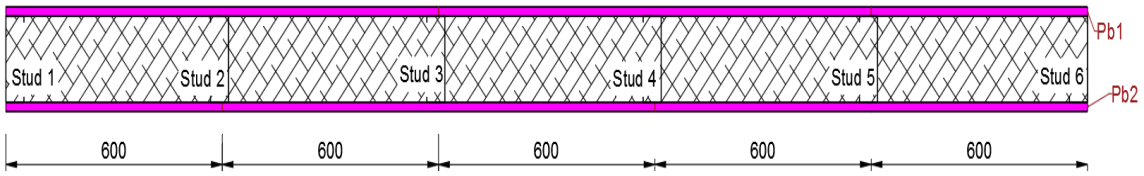

Figure 28: Cavity insulated and plasterboard lined LSF wall

- **Results of the model number 2**

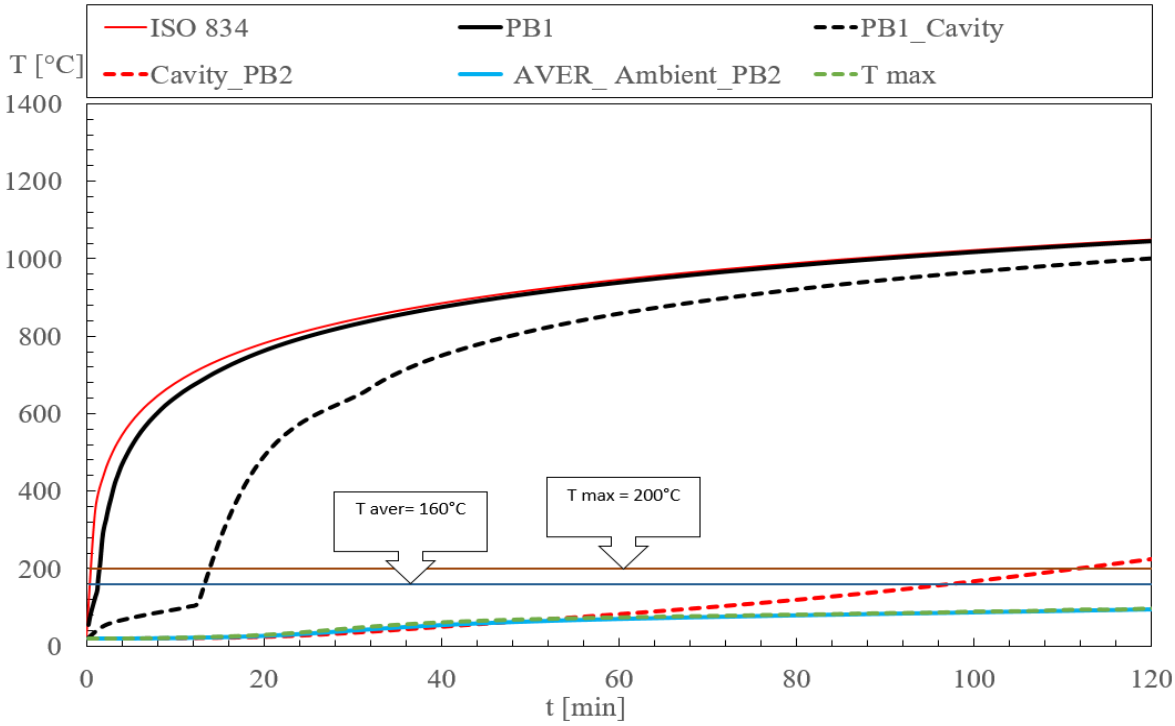

Figure 29: Average temperature variation results from the parametric analysis of model **2**

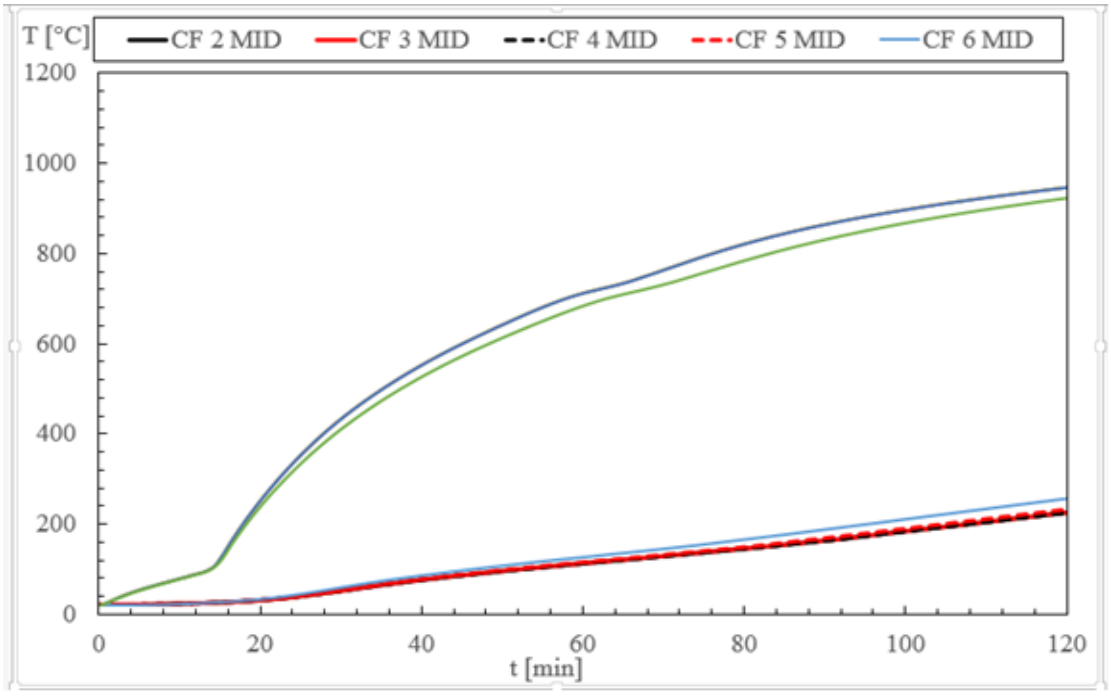

Figure 30: Numerical results for the parametric analysis on mid cold flanges

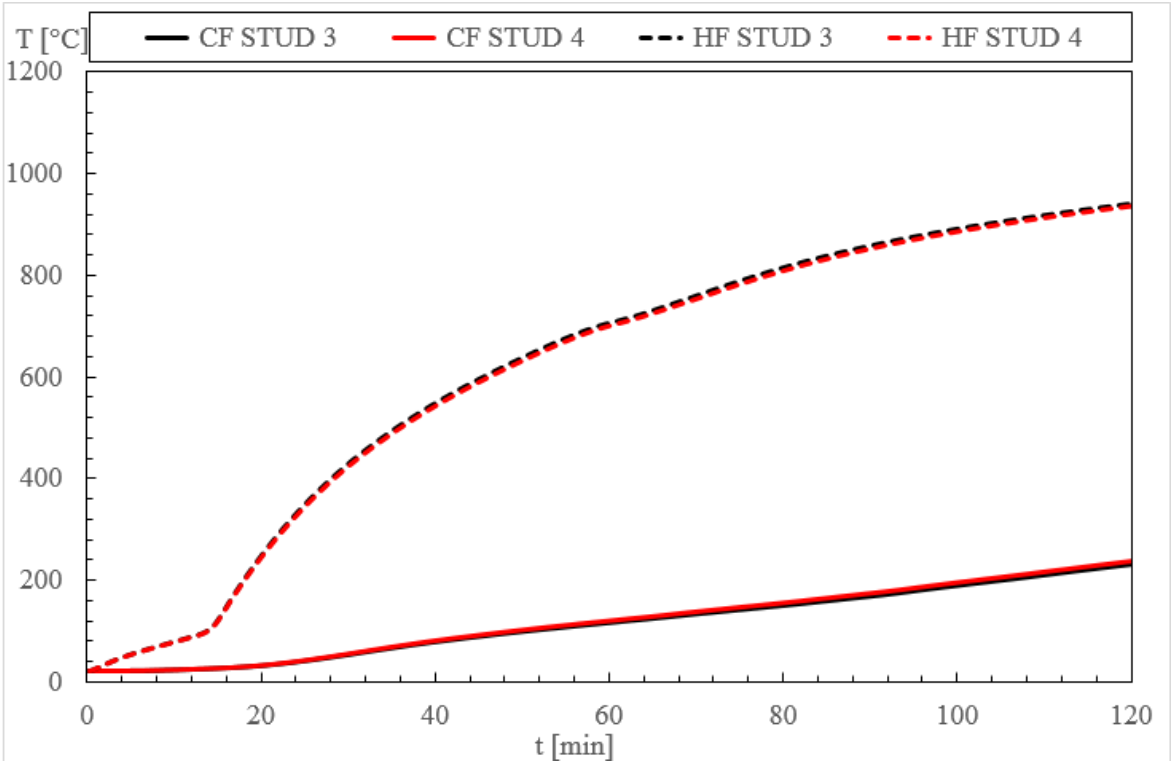

Figure 31: Numerical results for the parametric analysis on mid hot flanges

The numerical solution results of the LSF wall under fire ISO 834 standard condition are demonstrated in the Figure 29. The fire resistance was determined by the average temperature (160°C), the failure time of this model was at the minute 175, while the criteria for the maximum temperature(200°C) was satisfied after 181 minutes.

From this simulation we can note that the additional Gypsum layer improved strongly the fire resistance.

Table 5: Parametric analysis configurations and the fire filler time

Case	TH_ steel [mm]	TH_ cavity [mm]	TH_plates [number thickness plates]	Schematics	Fire resistance [min] (I)
01	1.15	92	2X16	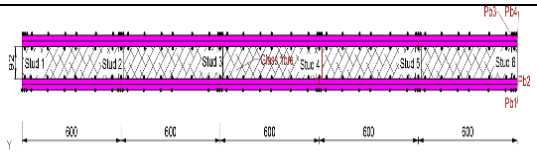	111
02	1	150	1X16	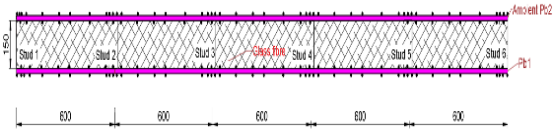	175

Chapter 6: Conclusions and Future Work

6.1. Conclusions

This thesis illustrated a study about the fire behaviour of the LSF non load bearing wall being under fire standard curve, using the validation of fire test done by Anthony Deloge Ariyanayagam, Mahen Mahendran [15]

A different step was mentioned for the aim of having a 3D of the LSF wall on the ANSYS program and simulating a real full fire test, applying different material properties.

Also, two parametric analysis have been developed with different configurations and dimensions.

A numerical comparison has been done in between the numerical and experimental results on the average temperature values of different region on the LSF wall such as the fire side, the bottom cavity and the top one plus the unexposed side using the Root Mean Square (RMS) formula.

Another comparison was done by the absolute relative error between the fire resistances obtained by the numerical and experimental fire test done by Anthony Deloge Ariyanayagam, Mahen Mahendran [15] .

The numerical results (Fire resistance I) agreed well with the experimental one.

The parametric analysis results showed that the increment of the number of protection plaster board had a good effect on the fire behavior of the LSF wall with improving it's fire resistance.

Also, it was strongly noted from the model number 2 that bigger cavity thickness gives higher fire resistance

.

From this parametric analysis study, we can conclude that the best solution to have a great fire resistance is to have a big thickness of an insulated cavity on the wall.

6.2. Future work

More 3D numerical models with different configuration are proposed on the cavity (empty or full), different insulation material to be applied on the cavity, also its thickness, a different studs dimensions.

3D numerical models (thermal and structure) also can be devolved on the future work. A series of standard full fire test can be developed.

References

[1] Sultan MA. A model for predicting heat transfer through noninsulated unloaded steel-stud gypsum board wall assemblies exposed to fire.1996,Fire Technol;32:239–59. https://doi.org/10.1007/bf01040217.

[2] Alfawakhiri F, Sultan MA, MacKinnon DH. Fire resistance of loadbearing steel-stud walls protected with gypsum board: A review. 1999, Fire Technol;35:308–35. https://doi.org/10.1023/A:1015401029995.

[3] Alfawakhiri F, Sultan MA. Fire resistance of loadbearing LSF assemblies. Int Spec Conf Cold-Formed Steel Struct Recent Res Dev Cold-Formed Steel Des Constr 2000:545–61.

[4] Kodur VKR, Sultan MA. Factors influencing fire resistance of load-bearing steel stud walls. 2006, Fire Technol;42:5–26. https://doi.org/10.1007/s10694-005-3730-y.

[5] Uvsløkk S, Arnesen H. Thermal insulation performance of reflective material layers in well insulated timber frame structures. 2008, 8Th Symp Build Phys Nord Ctries:1–8.

[6] Shahbazian A, Wang YC. Direct Strength Method for calculating distortional buckling capacity of cold-formed thin-walled steel columns with uniform and non-uniform elevated temperatures.2012, Thin-WalledStruct;53:188–99. https://doi.org/10.1016/j.tws.2012.01.006.

[7] Shahbazian A, Wang YC. A simplified approach for calculating temperatures in axially loaded cold-formed thin-walled steel studs in wall panel assemblies exposed to fire from one side. 2013,Thin-Walled Struct ;64:60–72. https://doi.org/10.1016/j.tws.2012.12.005.

[8] Faculty of Engineering Department : Division of Fire Safety Engineering Year 2015-2016 Reliability of fire barriers Jonathan Vallée Promoter : Patrick Van Hees Master thesis submitted in the Erasmus Mundus Study Programme International Master of Science i 2016.

[9] Piloto PAG, Khetata MS GA. Fire performance of non-load bearing light steel framing walls –numerical simulation. 2017,Sereal Untuk ;51:1603–1610.

[10] Khetata M, Fernandes L, Piloto P, Razuk H. fire resistance of non-loadbearing light steel framing walls : numerical validation n.d.

[11] Piloto PAG, Khetata MS, Gavilán ABR. Fire Performance of Non-Loadbearing Light Steel Framing Walls – Numerical and Simple Calculation Methods.2017, MATTER Int J Sci Technol;3:13–23. https://doi.org/10.20319/mijst.2017.33.1323.

[12] Piloto P. Fire resistance of cold-formed steel walls with mixed panels: Results from isolation rating (I) and loadbearing prediction rating (R). 2018, Metálica:12–7. https://doi.org/10.30779/cmm_metalica_mi07_02.

[13] Piloto PAG, Khetata MS, Gavilán ABR. Loadbearing Capacity of Lsf Walls Under Fire Exposure.2018,MATTER Int J Sci Technol;4:104–24. https://doi.org/10.20319/mijst.2018.43.104124.

[14] Paulo Piloto, Khetata M, Gavilán A. Fire Resistance Tests of Non-Loadbearing LSF Walls. TEST&E 2019 - 2nd Conf Test Exp Civ Eng - Proc 2019:429–40.

[15] Ariyanayagam AD, Mahendran M. Fire performance of load bearing LSF wall systems made of low strength steel studs.2018 Thin-Walled Struct;130:487–504. https://doi.org/10.1016/j.tws.2018.05.018.

[16] LSK E. European Lightweight Steel-framed Construction. 2005,Arcelor:92.

[17] Magarabooshanam H, Ariyanayagam A, Mahendran M. Fire resistance of non-load bearing LSF walls with varying cavity depth. 2020,Thin-Walled Struct;150:106675. https://doi.org/10.1016/j.tws.2020.106675.

[18] Standard I. Iso 834-1 1999;1999.

[19] Bsi. BSI Standards Publication Fire resistance tests Part 1 :2012General Requirements.

[20] Mitin II. European standard. Tselliuloza, Bum Karton/Pulp, Pap Board 2004:18-22+95. https://doi.org/10.1088/0031-9112/25/4/007.

[21] Spalding DB. Handbook of heat transfer. vol. 18. 1975. https://doi.org/10.1016/0017-9310(75)90148-9.

[22] ANSYS. Academic research mechanical (Release 18.2),